

## Article

# A Novel Zero Watermarking Based on DT-CWT and Quaternion for HDR Image

Jiangtao Huang <sup>1,2</sup>, Shanshan Shi <sup>1</sup>, Zhouyan He <sup>1,2</sup> and Ting Luo <sup>1,2,\*</sup> 

<sup>1</sup> Faculty of Information Science and Engineering, Ningbo University, Ningbo 315211, China; Hitgen@163.com (J.H.); 1912082153@nbu.edu.cn (S.S.); hezhouyan@nbu.edu.cn (Z.H.)

<sup>2</sup> College of Science and Technology, Ningbo University, Ningbo 315212, China

\* Correspondence: luoting@nbu.edu.cn; Tel.: +86-13567436129

**Abstract:** This paper presents a high dynamic range (HDR) image zero watermarking method based on dual tree complex wavelet transform (DT-CWT) and quaternion. In order to be against tone mapping (TM), DT-CWT is used to transform the three RGB color channels of the HDR image for obtaining the low-pass sub-bands, respectively, since DT-CWT can extract the contour of the HDR image and the contour change of the HDR image is small after TM. The HDR image provides a wide dynamic range, and thus, three-color channel correlations are higher than inner-relationships and the quaternion is used to consider three color channels as a whole to be transformed. Quaternion fast Fourier transform (QFFT) and quaternion singular value decomposition (QSVD) are utilized to decompose the HDR image for obtaining robust features, which is fused with a binary watermark to generate a zero watermark for copyright protection. Furthermore, the binary watermark is scrambled for the security by using the Arnold transform. Experimental results denote that the proposed zero-watermarking method is robust to TM and other image processing attacks, and can protect the HDR image efficiently.



check for updates

**Citation:** Huang, J.; Shi, S.; He, Z.; Luo, T. A Novel Zero Watermarking Based on DT-CWT and Quaternion for HDR Image. *Electronics* **2021**, *10*, 2385. <https://doi.org/10.3390/electronics10192385>

Academic Editor: Chiman Kwan

Received: 28 August 2021

Accepted: 27 September 2021

Published: 29 September 2021

**Publisher's Note:** MDPI stays neutral with regard to jurisdictional claims in published maps and institutional affiliations.



**Copyright:** © 2021 by the authors. Licensee MDPI, Basel, Switzerland. This article is an open access article distributed under the terms and conditions of the Creative Commons Attribution (CC BY) license (<https://creativecommons.org/licenses/by/4.0/>).

**Keywords:** zero-watermarking; DT-CWT; QFFT; QSVD; tone mapping

## 1. Introduction

Since high dynamic range (HDR) imaging is able to capture the wide range of real-world lighting, the HDR image meets the high requirements for image quality and visual perception [1–3]. At present, the HDR image can be found in many applications, such as computer vision, broadcasting, surveillance, Internet of things (IOT), and so on [4,5]. However, during the transmission process, the HDR image may be copied and stolen by unauthorized users, and their copyright needs to be protected. Watermarking is security technology that can embed the copyright information into the HDR image for image protection [6,7].

Traditional watermarking methods need to embed a watermark into the original image, which will cause some damage to some extent [8,9]. However, any minor modification is not allowed on some special applications, such as military and judicial imaging. Thus, zero watermarking is proposed by mining key image features to obtain watermarking robustness without image distortion [10]. Hence, it can solve the contradiction between watermarking robustness and imperceptibility. Zhou et al. decomposed the image by using discrete wavelet transform (DWT), and then each DWT transformed block was decomposed by using SVD [11]. The maximum singular value was utilized to form a zero-watermark sequence with the copyright information. However, correlations of zero-watermark sequences constructed from different images are high, which means the uniqueness verification of zero watermark for different images is low. In order to increase uniqueness verification of zero watermark, Rao et al. used enhance SVD to generate a zero watermark [12]. Gao et al. used Bessel–Fourier with rotation invariance to compute a zero watermark, and the method was robust to compression, noise, and rotation

attacks [13]. Han et al. decomposed the image by using non-subsampled shearlet transform (NSST), and then, each block was performed with LU decomposition to construct a zero watermark [14]. However, the above zero-watermarking methods were only designed for gray-scale images.

The color image has a rich color information, and its color channels have strong correlations, which can be mined for robust characteristics of the image. Zhu et al. designed a Schur and Contourlet transform based zero watermarking for the color image, but a zero watermark was constructed only in YCoCg space of the color image [15]. Zheng et al. utilized DWT and SVD to decompose RGB channels of the color image, respectively, for constructing a zero watermark, but correlations of three channels were missed [16]. To preserve the relationships of the three channels for extracting robust features, many researchers introduced multi-dimensional transformations, such as tensor and quaternion. In order to resist geometric attacks, Wang et al. selected quaternion-robust exponent moments (QEMs) of the color image to generate a zero watermark [17]. Yang et al. designed a computational strategy for fast generalized extreme complex exponential transform (QGPCET), and selected the mixed low-order moments in QGPCET coefficients to construct a zero watermark [18]. Jiang et al. constructed two three-dimensional tensors using R, G, B and gray channels and expanded them, respectively [19]. By performing SVD and DCT on the expanded matrix, the features representing the main information of the image were extracted to construct a robust zero watermark. However, the above zero-watermarking methods are all designed for the LDR image, and if they are directly applied in the HDR image, the special HDR image characteristics will be ignored for resisting special image attacks, such as tone mapping (TM). Since the HDR image has a wide dynamic range, the inner relationship of one channel is decreased. Moreover, most existing display devices are still used for LDR images, and have a limited dynamic range, and thus, the HDR image should be tone mapped [20,21]. Therefore, TM is an undoubtedly unique and inevitable image processing for HDR image watermarking to be considered when copyright of the HDR image should be protected.

Recently, some robust HDR image watermarking methods were researched. Guerrini et al. used DWT to decompose the image, and then utilized quantized exponential modulation (QEM) to embed the watermark [22]. However, the robustness of that method was not high. Solachidis et al. successively embedded a watermark into LDR image sequences with different exposures in the DWT domain [23]. The idea of embedding a watermark many times obtains high robustness, but it causes the decline of invisibility at the same time. Considering that the structure of the image is stable after TM processing, nonsubsampling contourlet transform and SVD were successively operated on the HDR image to extract the associated structural features for data embedding [24]. Moreover, a hybrid perceptual mask was used to increase the imperceptibility. In order to mine strong correlations of the HDR image, Luo et al. used Tucker decomposition to transform the HDR image to embed a robust watermark, which is robust to varieties of TM attacks [25]. However, the above HDR image watermarking methods need to obtain high robustness, and the corresponding visual quality is decreased. To achieve the tradeoff between watermarking robustness and invisibility, the HDR image zero watermarking is suitable to copyright protection of the HDR image without any quality distortion.

TM processing on the HDR image causes loss of color, brightness, and texture [26], and thus, features extracted from the HDR image should resist those large changes for the zero-watermark construction. In general, after TM, the contour of the HDR image changes a little, and it can be extracted by performing dual tree complex wavelet transform (DT-CWT) [27]. In this paper, a novel zero-watermarking method based on DT-CWT, quaternion fast Fourier transform (QFFT), and quaternion singular value decomposition (QSVD) for the HDR image is presented. For extracting robust contour information, RGB channels are decomposed by DT-CWT to compute three low-pass sub-bands, respectively. In order to mine correlations of three channels, those three low-pass sub-bands are considered as a whole to be transformed by using QFFT and QSVD to compute the largest singular value

for extracting robust features. The XOR operation is applied between robust features and the copyright watermark to generate a zero watermark. Experimental results prove that the proposed method is robust to TM and image processing attacks.

The main contributions of the paper are listed as follows.

1. A novel robust DT-CWT-, QFFT-, and QSVD-based zero-watermarking method for the HDR image is presented.
2. Since the contour of the HDR image has not changed much after TM operation, DT-CWT is used to extract the contour information.
3. Three color channels of the HDR image are considered as a whole to be transformed by using QFFT and QSVD for extracting robust image features.

The remainder of the paper is organized as follows. DT-CWT, QFFT, and QSVD are introduced in Section 2. The proposed zero-watermarking method for the HDR image is depicted in Section 3. The experimental results and discussion are given in Section 4. In Section 5, we draw a conclusion.

## 2. Preliminary

In this section, DT-CWT, QFFT, and QSVD are introduced.

### 2.1. Dual Tree Complex Wavelet Transform (DT-CWT)

DT-CWT is an enhancement of DWT [27], and it has the properties of shift invariance and multi-directions. Two independent wavelet filter trees are operated on the same original signal, and two real dual tree wavelet coefficients are used to compute complex wavelet coefficients:

$$F_a + F_b i \tag{1}$$

where  $i$  is the imaginary operator,  $F_a$  and  $F_b$  are coefficients of two trees, respectively, and these coefficients generate six directionally selective sub-bands at approximately  $\pm 15^\circ$ ,  $\pm 45^\circ$ , and  $\pm 75^\circ$ .

Figure 1 shows that the two-dimensional signal is decomposed by using four-level DT-CWT. For the structure of DT-CWT,  $F_l^L$  is the low-pass sub-band, and  $F_{l,D}^H$  is the  $d^{th}$  high-pass sub-band, where  $l$  is the level of transformation,  $l = 1, 2, 3, 4$ ,  $d$  represents the direction, and  $d = 1, 2, 3, 4, 5, 6$ . When we decompose three color channels of the HDR image by using four-level DT-CWT, three low-pass sub-bands are computed and denoted as  $F_{4,R}^L$ ,  $F_{4,G}^L$ , and  $F_{4,B}^L$ , respectively. Figure 2 shows three low-pass sub-bands of the original HDR image ‘Rend13’, and it is clearly seen that the low-pass sub-bands show the main contour information of the image. Moreover, the low-pass band is invariant to small geometric change. Thus, it can be used to compute stable features for robust zero watermarking.

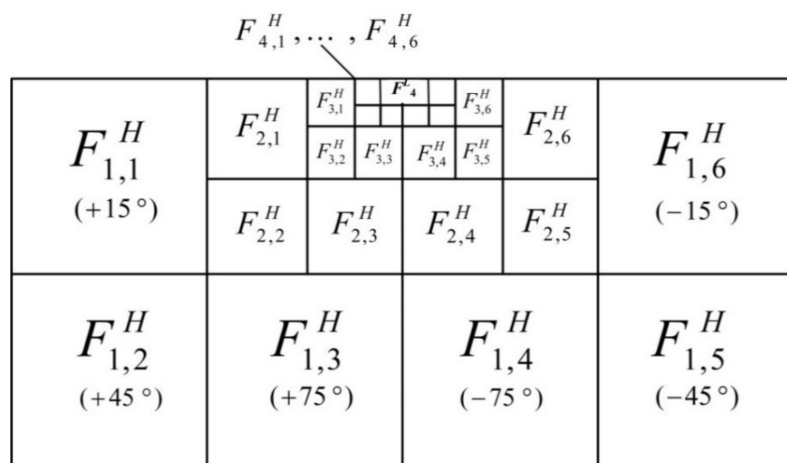


Figure 1. Four-level DT-CWT decomposition.

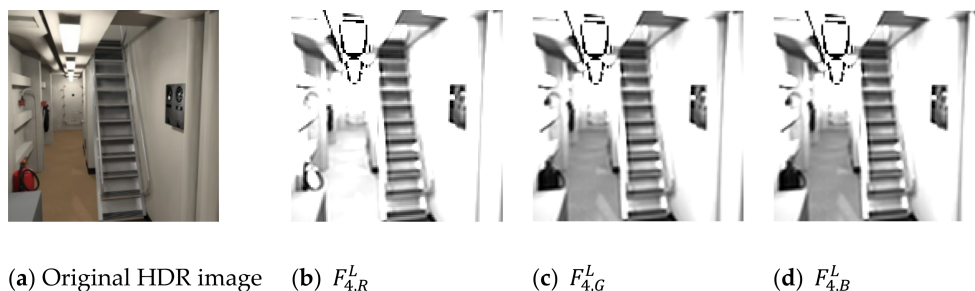


Figure 2. Low-pass sub-bands after four-level DT-CWT.

2.2. Quaternion Fast Fourier Transform (QFFT)

Before introducing QFFT, the quaternion is represented as the generalization of a complex number, and it can be denoted as:

$$q = q_r + q_i i + q_j j + q_k k \tag{2}$$

where  $i, j,$  and  $k$  are imaginary operators and  $q_r, q_i, q_j,$  and  $q_k$  are real.

When three low-pass sub-bands are extracted for the color HDR image, to mine correlations of three channels, they can be used to represent the whole image in quaternion form as:

$$F_4^L = F_{4,R}^L i + F_{4,G}^L j + F_{4,B}^L k \tag{3}$$

where the real value is set to 0.

In 1996, Sangwine was the first to propose the quaternion Fourier transform applied in the three-dimensional matrices [28]. For the  $F_{4,R}^L(a,b)$ , where  $(a,b)$  is the coefficient location in the low-pass sub-band, its generalized fast Fourier transform (FFT) and its reverse are as follows:

$$K_R(s,t) = \frac{1}{\sqrt{MN}} \sum_{a=0}^{M-1} \sum_{b=0}^{N-1} e^{-\mu 2\pi(\frac{as}{M} + \frac{bt}{N})} F_{4,R}^L(a,b) \tag{4}$$

$$F_{4,R}^L(a,b) = \frac{1}{\sqrt{MN}} \sum_{s=0}^{M-1} \sum_{t=0}^{N-1} e^{\mu 2\pi(\frac{as}{M} + \frac{bt}{N})} K_R(s,t) \tag{5}$$

where  $M$  and  $N$  are the width and length of the low-pass sub-band, respectively,  $\mu$  is unit pure quaternion,  $\mu^2 = -1$ , and  $\mu = (i + j + k) / \sqrt{3}$ .

Similarly,  $F_{4,G}^L$  and  $F_{4,B}^L$  can be transformed by using FFT to obtain  $K_G$  and  $K_B$ , respectively:

$$K_G(s,t) = FFT(F_{4,G}^L) = \frac{1}{\sqrt{MN}} \sum_{a=0}^{M-1} \sum_{b=0}^{N-1} e^{-\mu 2\pi(\frac{as}{M} + \frac{bt}{N})} F_{4,G}^L(a,b) \tag{6}$$

$$K_B(s,t) = FFT(F_{4,B}^L) = \frac{1}{\sqrt{MN}} \sum_{a=0}^{M-1} \sum_{b=0}^{N-1} e^{-\mu 2\pi(\frac{as}{M} + \frac{bt}{N})} F_{4,B}^L(a,b) \tag{7}$$

Considering three low-pass sub-bands of the HDR color image as a whole, the quaternion fast Fourier transform (QFFT) of  $F_4^L$  and its reverse are:

$$K(s,t) = (K_R(s,t))i + (K_G(s,t))j + (K_B(s,t))k \tag{8}$$

$$F_4^L(a,b) = (F_{4,R}^L(a,b))i + (F_{4,G}^L(a,b))j + (F_{4,B}^L(a,b))k \tag{9}$$

2.3. Quaternion Singular Value Decomposition (QSVD)

For any quaternion matrix  $B$ , an efficient SVD is proposed by Sangwine et al. [29], and a bidiagonal matrix  $Y$  is computed by bidiagonalizing  $B$  with quaternion Householder

transformations and a simple recursive technique. The singular values of  $Y$  and  $B$  are same, and the bidiagonalization of  $B$  can be represented by:

$$RBW = Y \tag{10}$$

where  $R$  and  $W$  are the left and right quaternion Householder matrices, respectively. Because  $R$  and  $W$  are unitary, it satisfies:  $Y = \bar{R}^T B \bar{W}^T$ . Suppose  $U$  and  $V$  are orthogonal matrices, and the SVD of  $Y$  can be presented by  $Y = USV^T$ . Thus, the SVD of quaternion matrix  $B$  is computed as follows:

$$A = \bar{H}^T USV^T \bar{G}^T \tag{11}$$

where  $\bar{H}^T U$  and  $V^T \bar{G}^T$  are unitary matrices,  $S = D(\sigma_1, \sigma_2, \dots, \sigma_n)$ ,  $\sigma_1 \geq \sigma_2 \geq \dots \geq \sigma_n$  are eigenvalues of  $B$ ,  $n$  is the singular number, and  $D(\bullet)$  constructs a diagonal matrix. The singular values represent the main correlations of the given matrix. In particular, the maximum singular value  $\sigma_1$  contains the main energy and has strong stability.

Since QFFT and QSVD combine three channels to be transformed, strong correlations of the HDR color image are maintained for robust zero watermarking.

### 3. Proposed HDR Image Zero Watermarking

In this section, a novel DT-CWT and quaternion-based zero watermarking for the HDR image is described. The binary watermark as the copyright information is denoted as  $W$  with the size of  $P \times P$ , and three RGB channels are denoted as  $f_R$ ,  $f_G$ , and  $f_B$ , respectively. The detailed processes of zero-watermark construction and verification are depicted, respectively.

#### 3.1. Construction of Zero Watermark

The processes of zero-watermark construction are illustrated in Figure 3.

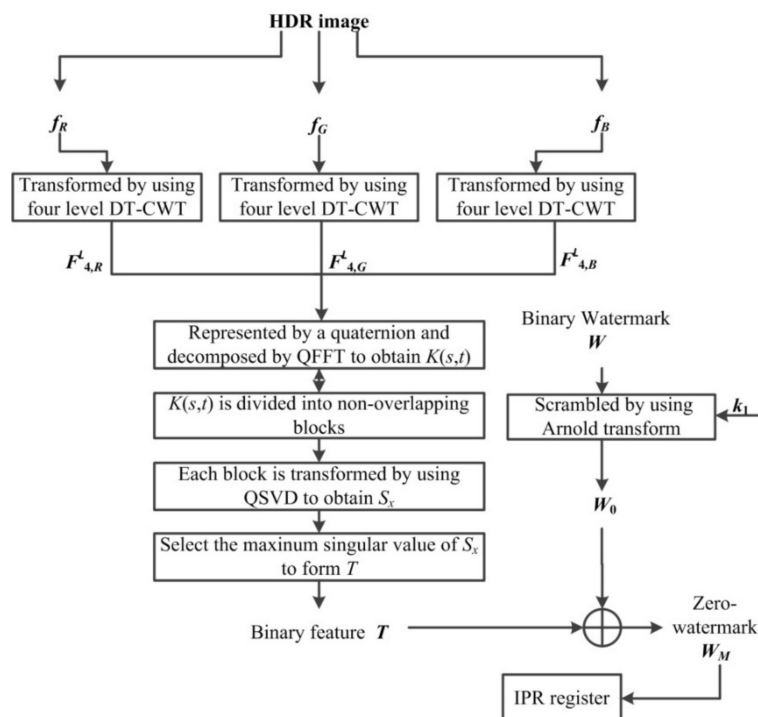


Figure 3. Flowchart of zero-watermark construction.

Step a-1. With a private key, the Arnold transform is utilized to scramble  $W$  to obtain  $W_0$ :

$$W_0 = \text{Arnold}(W) \tag{12}$$

where  $\text{Arnold}(\bullet)$  is the Arnold transform.

Step a-2.  $f_R, f_G,$  and  $f_B$  are decomposed by using four-level DT-CWT to obtain  $F_{4,R}^L, F_{4,G}^L,$  and  $F_{4,B}^L,$  respectively.

Step a-3.  $F_{4,R}^L, F_{4,G}^L,$  and  $F_{4,B}^L$  are combined and represented in a pure quaternion  $F_4^L,$  and QFFT is applied on  $F_4^L$  to obtain  $K(s, t).$

Step a-4.  $K(s, t)$  is divided into non-overlapping blocks  $B_x,$  where  $x$  is the block index and its size is  $c \times c.$  Only  $P \times P + 1$  blocks are randomly selected to construct a zero watermark with private key  $k_2.$  The diagonal matrix  $S_x$  is computed by applying QSVD on  $B_x,$  and  $\sigma_{1,x}$  of each block is extracted.

Step a-5. All maximum singular values  $\sigma_{1,x}$  of all blocks are computed, and then the feature matrix  $T$  is calculated by comparing  $\sigma_{1,x}$  and  $\sigma_{1,x+1}$ :

$$T_x = \begin{cases} 1 & \text{if } \sigma_{1,x+1} > \sigma_{1,x} \\ 0 & \text{others} \end{cases} \tag{13}$$

Step a-6. Zero watermark  $W_M$  is computed:

$$W_M = T \oplus W_0 \tag{14}$$

Step a-7. For protecting copyright,  $W_M, k_1$  and  $k_2$  are registered in a third-part intellectual property rights (IPR) database.

### 3.2. Verification of Zero Watermark

Figure 4 shows processes of zero-watermark extraction for copyright verification, which is symmetric to the zero-watermark construction. Let  $f^*$  be the HDR image to be verified, which may be under some image attacks.

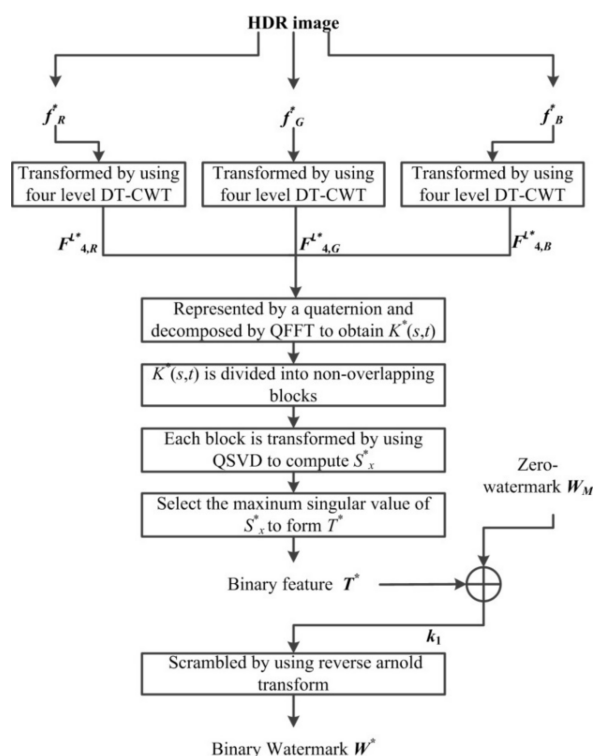


Figure 4. Flowchart of zero-watermark verification.

Step b-1. Four-level DT-CWT is used to decompose the three channels of  $f^*$  to obtain three low-pass sub-bands, denoted as  $F_{4,R}^{L*}$ ,  $F_{4,G}^{L*}$ , and  $F_{4,B}^{L*}$  respectively.

Step b-2.  $F_{4,R}^{L*}$ ,  $F_{4,G}^{L*}$ , and  $F_{4,B}^{L*}$  are combined as a pure quaternion  $F_4^{L*}$ , which is transformed by using QFFT to compute  $K^*(u, v)$ .

Step b-3.  $K^*(u, v)$  is divided into non-overlapping blocks  $B_x^*$ , and  $P \times P + 1$  blocks are selected to compute a zero watermark with the private key  $k_2$ .  $B_x^*$  is decomposed by using QSVD to compute the diagonal matrix  $S_x^*$ , and its maximum singular value  $\sigma_{1,x}^*$  of each block is calculated.

Step b-4. The feature matrix  $T^*$  is constructed by comparing  $\sigma_{1,x}^*$  and  $\sigma_{1,x+1}^*$ :

$$T_x^* = \begin{cases} 1 & \text{if } \sigma_{1,x+1}^* > \sigma_{1,x}^* \\ 0 & \text{others} \end{cases} \quad (15)$$

Step b-5.  $W_M$  and  $T^*$  are computed by using the exclusive-or operation to obtain  $W_0^*$ :

$$W_0^* = T^* \oplus W_M \quad (16)$$

Step b-6. The inverse Arnold transform is performed on  $W_0^*$  to compute  $W^*$ .

Step b-7.  $W^*$  and  $W$  are compared for the copyright verification.

The proposed watermarking method is designed for HDR images in RGB format since the three RGB channels have strong correlations, which can be mined for robust features. However, the proposed method is not suitable for other color formats, and especially not the three-color channel formats, such as LHS format.

#### 4. Experimental Results and Discussions

Eight HDR images are used to be tested as illustrated in Figure 5, and the binary watermark is illustrated in Figure 6. The robustness is evaluated by the bit error rate (BER) [30] is defined as follows:

$$BER = \frac{N_e}{N_t} \quad (17)$$

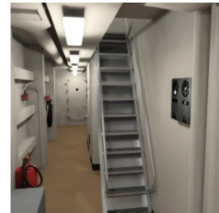
where  $N_e$  is the wrong bits number of the extracted watermark and  $N_t$  is the correct bits number of the watermark.



(a) Rend08 (800 × 1000)



(b) Apartment (1536 × 2048)



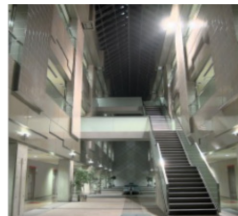
(c) Rend09 (1024 × 1024)



(d) Rend10 (1024 × 1024)



(e) Rend13 (1024 × 1024)



(f) AtriumNight (1016 × 760)



(g) Bottles (512 × 1024)



(h) Rend01 (1024 × 1024)

Figure 5. Original HDR images.



**Figure 6.** Original watermark (64 × 64).

#### 4.1. Zero-Watermark Uniqueness

A zero watermark generated from one HDR image should be unique and irrelevant to other HDR images for copyright protection. Normalized cross-correlation (*NC*) is utilized to compute the difference between two zero-watermark images:

$$NC = \frac{\sum_i \sum_j W_1(i, j) W_2(i, j)}{\sqrt{\sum_i \sum_j W_1^2(i, j)} \sqrt{\sum_i \sum_j W_2^2(i, j)}} \quad (18)$$

where  $W_1$  and  $W_2$  represent two zero-watermark images, respectively.

Table 1 shows the *NC*s of zero-watermark images. The maximum *NC* is less than 0.6, which denotes that the zero watermark from one HDR image is distinguishable from those of other images and can prove the uniqueness of a zero watermark.

**Table 1.** *NC*s between generated zero-watermark images [%].

Image	Rend08	Apartment	Rend09	Rend10	Rend13	AtriumNight	Bottles	Rend01
Rend08	100.00	51.42	50.63	53.85	51.76	50.64	52.16	54.21
Apartment	51.42	100.00	56.43	54.91	57.61	54.26	50.10	54.59
Rend09	50.63	56.43	100.00	52.70	54.46	52.35	54.04	54.32
Rend10	53.85	54.91	52.70	100.00	53.00	52.16	54.04	49.56
Rend13	51.76	57.61	54.46	53.00	100.00	50.26	53.89	55.02
AtriumNight	50.64	54.26	52.35	52.16	50.26	100.00	54.30	52.41
Bottles	52.16	50.10	54.04	54.04	53.89	54.30	100.00	53.52
Rend01	54.21	54.59	54.32	49.56	55.02	52.41	53.52	100.00

#### 4.2. Robustness of Zero Watermarking

In order to show the robustness of the proposed method, TM and common image processing are used for testing.

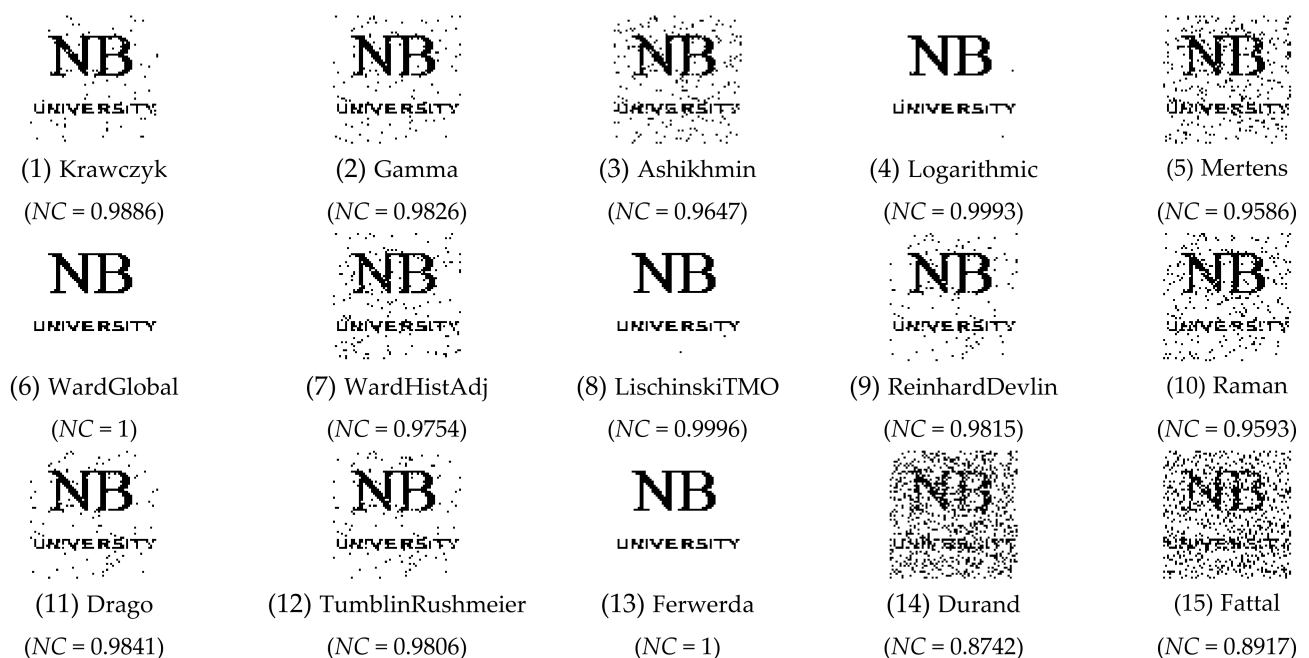
##### 4.2.1. Robustness on TM Attack

*BER*s of the proposed method for eight images attacked by 15 different TMs are computed, as shown in Table 2. It is clearly seen that for most of the TM attacks, all *BER*s of the proposed method are lower than 0.75, which reflects the efficiency of the copyright protection. For Durand and Fattal TM attacks, most of the *BER*s are a little higher than those of other TMs, and but can still play an important role in copyright protection. Moreover, the average *BER*s of all TMs are all lower than 0.08, which proves the high robustness of the proposed method for the TM attack.

Figure 7 shows watermark extraction, when Rend01 is attacked by different TMs. Obviously, from the extracted watermark, we can know the copyright of the HDR image. Moreover, we can see that the corresponding *NC* is high, which means that the extracted watermark is similar to the original watermark. This is mainly because DT-CWT can extract the contour information, and QFFT and QSVD mine strong correlations of the HDR image efficiently.

**Table 2.** BERs of HDR images while under TM attacks [%].

	Rend08	Apartment	Rend09	Rend10	Rend13	AtriumNight	Bottles	Rend01
Krawczyk	8.64	13.67	1.39	10.81	0.08	2.37	9.50	2.00
Gamma	8.18	13.33	3.08	4.59	5.96	5.37	6.32	3.05
Ashikhmin	6.86	7.93	6.84	10.82	7.42	8.54	11.04	6.13
Logarithmic	1.51	1.81	1.10	2.34	3.05	2.22	1.73	0.12
Mertens	10.18	13.38	4.13	9.21	8.42	7.79	10.42	6.45
WardGlobal	0.00	0.00	0.83	1.68	2.32	1.56	0.00	0.00
WardHistAdj	3.22	3.64	4.52	4.00	5.30	5.86	5.30	4.27
LischinskiTMO	2.03	7.13	1.98	3.27	4.88	3.15	4.96	0.07
ReinhardDevlin	3.20	6.32	4.39	9.18	6.64	6.74	7.25	3.25
Raman	6.18	7.76	3.13	5.20	6.52	5.79	9.57	4.79
Drago	3.83	5.57	2.78	4.88	5.62	5.66	6.23	2.78
TumblinRushmeier	2.76	3.15	2.29	5.54	4.61	4.05	4.66	3.39
Ferwerda	0.02	0.22	0.12	0.27	0.09	0.12	0.71	0.00
Durand	14.94	16.39	17.60	20.27	19.51	16.28	15.43	17.65
Fattal	10.67	10.91	11.04	18.48	12.48	9.91	11.79	18.16
Average	5.48	7.41	4.34	7.36	6.59	5.69	6.99	4.18

**Figure 7.** Extracted watermark from Rend01 under different TMs.

#### 4.2.2. Robustness on Common Image Processing

To show the capability of resisting other attacks, some common image processing attacks are also used for testing, as listed in Table 3. Table 4 shows that the BERs of the eight HDR images are all less than 20%, which means that the proposed method has the ability of copyright protection for resisting common image processing attacks. Furthermore, averages of BER are all below 6% for all images, which again denotes the high robustness of the proposed method.

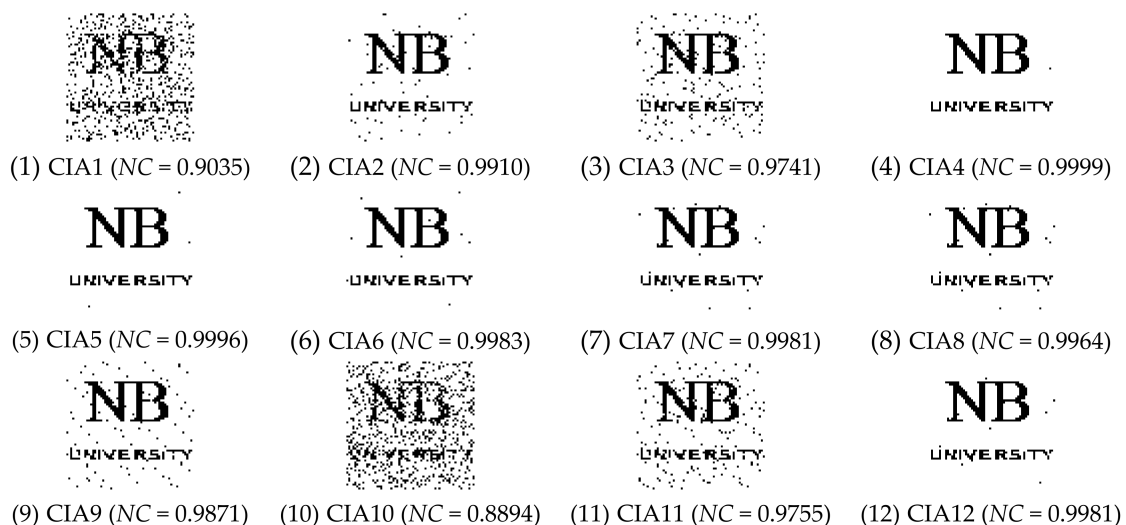
**Table 3.** List of common image processing attacks.

Number	Common Attacks	Number	Common Attacks
CIA1	‘Salt & Pepper’ (0.001)	CIA7	Poisson noise
CIA2	Median filter (3 × 3)	CIA8	Image sharpen (0.5)
CIA3	Median filter (5 × 5)	CIA9	Average filter (4 × 4)
CIA4	Scaling (4)	CIA10	Imrotate (2)
CIA5	Scaling (1/4)	CIA11	Gaussian noise
CIA6	Gaussian low-pass filter (3 × 3)	CIA12	Imadjust

**Table 4.** BERs of HDR images under common image processing [%].

	Rend08	Apartment	Rend09	Rend10	Rend13	AtriumNight	Bottles	Rend01
CIA1	5.40	10.79	3.74	8.42	8.67	5.30	7.13	10.87
CIA2	0.56	0.76	0.85	2.86	0.32	2.12	0.61	1.59
CIA3	1.73	1.59	1.81	3.66	0.90	4.22	1.90	4.52
CIA4	0.02	0.00	0.00	0.02	0.02	0.00	0.00	0.02
CIA5	0.02	0.00	0.00	0.04	0.05	0.00	0.00	0.07
CIA6	0.49	0.12	0.12	0.46	0.51	0.12	0.22	0.29
CIA7	6.01	10.30	1.37	2.12	4.20	2.49	2.37	0.34
CIA8	6.08	10.60	1.59	2.51	4.37	2.83	2.42	0.56
CIA9	0.90	0.44	0.46	1.34	1.20	0.34	0.98	2.27
CIA10	15.65	14.23	10.72	15.97	9.06	11.24	17.87	18.53
CIA11	2.59	2.37	1.71	2.86	2.39	2.39	2.81	4.27
CIA12	5.98	10.30	1.37	2.12	4.20	6.15	2.36	0.34
Average	4.86	5.83	2.67	4.43	2.99	4.31	4.32	3.87

After different image processing attacks were operated on Rend01, the watermark was extracted visually, as illustrated in Figure 8. All extracted watermark can be recognized for proving the copyright information. Similar results were obtained for other HDR images, and it proves that the proposed method can resist common image processing attacks well.

**Figure 8.** Extracted watermark from Rend01 under different image processing attacks.

### 4.3. Robustness Comparisons

In this section, Jiang's [19] and Bai's [24] methods were used and compared; moreover, under different TM attacks, corresponding *BERs* are computed, as shown in Table 5. Most *BERs* of the proposed method are less than those of other comparative methods. Although for Ashikhmin, Mertens, and Durand, the proposed method is a little lower than Bai's [24], and is worse than Jiang's [19] for WardGlobal, considering all TM attacks, the average *BER* is much lower than those of the other two methods. Thus, based on the above experimental results, the proposed method can obtain higher robustness and protect the HDR image more efficiently.

**Table 5.** Robustness comparisons on TM attacks [%].

Attack Type	Jiang's [19]	Bai's [24]	Proposed
	<i>BER</i>	<i>BER</i>	<i>BER</i>
Krawczyk	11.35	11.04	<b>6.80</b>
Gamma	12.29	12.34	<b>6.23</b>
Ashikhmin	16.49	<b>6.97</b>	8.19
Logarithmic	11.32	6.87	<b>1.73</b>
Mertens	16.55	<b>6.15</b>	8.74
WardGlobal	<b>0.53</b>	5.60	0.80
WardHistAdj	12.90	7.07	<b>4.51</b>
LischinskiTMO	12.87	5.38	<b>3.43</b>
ReinhardDevlin	14.80	11.99	<b>5.87</b>
Raman	17.65	9.64	<b>6.11</b>
Drago	12.84	6.85	<b>4.66</b>
TumblinRushmeier	12.15	8.09	<b>3.80</b>
Ferwerda	0.61	5.92	<b>0.19</b>
Durand	23.79	<b>6.66</b>	17.25
Fattal	16.74	13.89	<b>12.93</b>
Average	11.35	8.29	<b>6.08</b>

## 5. Conclusions

In this paper, based on dual tree complex wavelet transform (DT-CWT), quaternion fast Fourier transform (QFFT), and quaternion singular value decomposition (QSVD), a novel high dynamic range (HDR) image zero watermarking method has been presented. Since most tone mapping (TM) operations preserve the contour information of the image, the three RGB channels are transformed by using DT-CWT to extract low-pass sub-bands for the main contour, respectively. To extract the main correlations of the three channels of the HDR image, three low-pass sub-bands are considered as a whole to be decomposed by using QFFT, and are then divided into non-overlapping blocks. Each QFFT transformed block is decomposed by QSVD to obtain the maximum singular value for constructing a binary feature image, which is used with a binary watermark to generate a zero watermark. The experimental results prove that the proposed method has the ability to resist different TMs and image processing attacks, and is superior to the existing zero-watermarking methods. Since deep learning works well on feature extraction, in future research, we will use deep networks to mine features for constructing a robust zero watermark.

**Author Contributions:** Conceptualization, S.S.; Supervision, T.L.; Writing—original draft, J.H.; Writing—review and editing, J.H., S.S., Z.H. and T.L. All authors have read and agreed to the published version of the manuscript.

**Funding:** This research received no external funding.

**Institutional Review Board Statement:** Not applicable.

**Informed Consent Statement:** Not applicable.

**Acknowledgments:** This work was supported by the Natural Science Foundation of China under Grant No. 61971247. It was also sponsored by the K. C. Wong Magna Fund in Ningbo University.

**Conflicts of Interest:** The authors declare no conflict of interest.

## References

1. Liu, Z.; Lin, W.; Li, X.; Rao, Q.; Jiang, T.; Han, M.; Liu, S. ADNet: Attention-guided deformable convolutional network for high dynamic range imaging. In Proceedings of the IEEE/CVF Conference on Computer Vision and Pattern Recognition, Nashville, TN, USA, 19–25 June 2021; pp. 463–470.
2. Zhang, J.; Newman, J.P.; Wang, X.; Thakur, C.S.; Rattray, J.; Etienne-Cummings, R.; Wilson, M.A. A closed-loop, all-electronic pixel-wise adaptive imaging system for high dynamic range videography. *IEEE Trans. Circuits Syst. I Regul. Pap.* **2020**, *67*, 1803–1814. [[CrossRef](#)]
3. Woo, S.M.; Ryu, J.H.; Kim, J.O. Ghost-Free Deep High-Dynamic-Range Imaging Using Focus Pixels for Complex Motion Scenes. *IEEE Trans. Image Process.* **2021**, *30*, 5001–5016. [[CrossRef](#)] [[PubMed](#)]
4. Pan, Z.; Yu, M.; Jiang, G.; Xu, H.; Peng, Z.; Chen, F. Multi-exposure high dynamic range imaging with informative content enhanced network. *Neurocomputing* **2020**, *386*, 147–164. [[CrossRef](#)]
5. Huang, Y.; Qiu, S.; Wang, C.; Li, C. Learning Representations for High-Dynamic-Range Image Color Transfer in a Self-Supervised Way. *IEEE Trans. Multimed.* **2020**, *23*, 176–188. [[CrossRef](#)]
6. Fares, K.; Amine, K.; Salah, E. A robust blind color image watermarking based on Fourier transform domain. *Optik* **2020**, *208*, 164562. [[CrossRef](#)]
7. Hsu, L.Y.; Hu, H.T. Blind watermarking for color images using EMMQ based on QDFT. *Expert Syst. Appl.* **2020**, *149*, 113225. [[CrossRef](#)]
8. Hu, H.T.; Hsu, L.Y.; Chou, H.H. An improved SVD-based blind color image watermarking algorithm with mixed modulation incorporated. *Inf. Sci.* **2020**, *519*, 161–182. [[CrossRef](#)]
9. Ali, M.; Ahn, C.; Pant, M.; Kumar, S.; Singh, M.; Saini, D. An optimized digital watermarking scheme based on invariant DC coefficients in spatial domain. *Electronics* **2020**, *9*, 1428. [[CrossRef](#)]
10. Wen, Q.; Sun, T.; Wang, S. Concept and application of zero-watermark. *Acta Electron. Sin.* **2003**, *31*, 214–216.
11. Zhou, Y.; Jin, W. A novel image zero-watermarking scheme based on DWT-SVD. In Proceedings of the 2011 International Conference on Multimedia Technology, Hangzhou, China, 26–28 July 2011; pp. 2873–2876.
12. Rao, Y.R.; Nagabhooshanam, E. A novel image zero-watermarking scheme based on DWT-BN-SVD. In Proceedings of the International Conference on Information Communication and Embedded Systems (ICICES2014), Chennai, India, 27–28 February 2014; pp. 1–6.
13. Gao, G.; Jiang, G. Bessel-Fourier moment-based robust image zero-watermarking. *Multimed. Tools Appl.* **2015**, *74*, 841–858. [[CrossRef](#)]
14. Han, S.C.; Zhang, Z.N. A novel zero-watermark algorithm based on LU decomposition in NSST domain. In Proceedings of the 2012 IEEE 11th International Conference on Signal Processing, Beijing, China, 21–25 October 2012; Volume 3, pp. 1592–1596.
15. Zhu, C.W.; Li, Y.Y.; Chi, W.D.; Gao, S.; Fan, D. Zero-watermarking Algorithm for Color Image in Contourlet Domain Based on Schur Decomposition. *Inf. Technol. Informatiz.* **2019**, *2*, 89–93.
16. Zheng, Q.; Liu, N.; Cao, B.; Wang, F.; Yang, Y. Zero-watermarking algorithm in transform domain based on RGB channel and voting strategy. *J. Inf. Process. Syst.* **2020**, *16*, 1391–1406.
17. Wang, C.P.; Wang, X.Y.; Xia, Z.Q.; Zhang, C.; Chen, X.J. Geometrically resilient color image zero-watermarking algorithm based on quaternion exponent moments. *J. Vis. Commun. Image Represent.* **2016**, *41*, 247–259. [[CrossRef](#)]
18. Yang, H.Y.; Qi, S.R.; Niu, P.P.; Wang, X.Y. Color image zero-watermarking based on fast quaternion generic polar complex exponential transform. *Signal Process. Image Commun.* **2020**, *82*, 115747. [[CrossRef](#)]
19. Jiang, F.; Gao, T. A robust zero-watermarking algorithm for color image based on tensor mode expansion. *Multimed. Tools Appl.* **2020**, *79*, 7599–7614. [[CrossRef](#)]
20. Jia, Y.; Zhang, W. Efficient and adaptive tone mapping algorithm based on guided image filter. *Int. J. Pattern Recognit. Artif. Intell.* **2020**, *34*, 2054012. [[CrossRef](#)]
21. Mohammadi, P.; Pourazad, M.T.; Nasiopoulos, P. A Perception-based Inverse Tone Mapping Operator for High Dynamic Range Video Applications. *IEEE Trans. Circuits Syst. Video Technol.* **2020**, *31*, 1711–1723. [[CrossRef](#)]
22. Guerrini, F.; Okuda, M.; Adami, N.; Leonardi, R. High dynamic range image watermarking robust against tone-mapping operators. *IEEE Trans. Inf. Forensics Secur.* **2011**, *6*, 283–295. [[CrossRef](#)]
23. Solachidis, V.; Maiorana, E.; Campisi, P. HDR image multi-bit watermarking using bilateral-filtering-based masking. In *Image Processing: Algorithms and Systems XI*; International Society for Optics and Photonics: Bellingham, WA, USA, 2013; Volume 8655, p. 865505.

24. Bai, Y.; Jiang, G.; Yu, M.; Peng, Z.; Chen, F. Towards a tone mapping-robust watermarking algorithm for high dynamic range image based on spatial activity. *Signal Process. Image Commun.* **2018**, *65*, 187–200. [[CrossRef](#)]
25. Luo, T.; Jiang, G.; Yu, M.; Xu, H.; Gao, W. Robust high dynamic range color image watermarking method based on feature map extraction. *Signal Process.* **2019**, *155*, 83–95. [[CrossRef](#)]
26. Rana, A.; Singh, P.; Valenzise, G.; Dufaux, F.; Komodakis, N.; Smolic, A. Deep tone mapping operator for high dynamic range images. *IEEE Trans. Image Process.* **2019**, *29*, 1285–1298. [[CrossRef](#)]
27. Huan, W.; Li, S.; Qian, Z.; Zhang, X. Exploring Stable Coefficients on Joint Sub-bands for Robust Video Watermarking in DT CWT Domain. *IEEE Trans. Circuits Syst. Video Technol.* **2021**. [[CrossRef](#)]
28. Ell, T.A.; Sangwine, S.J. Hypercomplex Fourier transforms of color images. *IEEE Trans. Image Process.* **2006**, *16*, 22–35. [[CrossRef](#)]
29. Sangwine, S.J.; Le Bihan, N. Quaternion singular value decomposition based on bidiagonalization to a real or complex matrix using quaternion Householder transformations. *Appl. Math. Comput.* **2006**, *182*, 727–738. [[CrossRef](#)]
30. Wang, C.P.; Wang, X.Y.; Chen, X.J.; Zhang, C. Robust zero-watermarking algorithm based on polar complex exponential transform and logistic mapping. *Multimed. Tools Appl.* **2017**, *76*, 26355–26376. [[CrossRef](#)]